Adsorptive desulfurization of jet and diesel fuels using Ag/TiO$_x$–Al$_2$O$_3$ and Ag/TiO$_x$–SiO$_2$ adsorbents

A.H.M. Shahadat Hussain, Bruce J. Tatarchuk *

Center for Microfibrous Materials Manufacturing (CM3), Department of Chemical Engineering, Auburn University, Auburn, AL 36849, USA

HIGHLIGHTS

▶ Ag/TiO$_x$–Al$_2$O$_3$ and Ag/TiO$_x$–SiO$_2$ was effective in desulfurizing jet and diesel fuels.
▶ The supports enhanced capacity and extent of desulfurization at ambient conditions.
▶ TiO$_x$ dispersed mixed oxides increased surface area and hosted more silver oxides.
▶ Methyl groups attached to thiophenes hindered the adsorption onto sorbent surface.
▶ The greatest affinity was toward BT's while the least toward TMBT's and DMDBT's.

ARTICLE INFO

ABSTRACT

The objective of this work is to examine the performance of Ag/TiO$_x$–Al$_2$O$_3$ and Ag/TiO$_x$–SiO$_2$ for adsorptive desulfurization of JP5, JP8, Off-Road Diesel (ORD), and Ultra Low Sulfur Diesel (ULSD) at ambient conditions. These adsorbents were observed to be effective for desulfurizing liquid hydrocarbon feeds that ranged from 7.5 to 1172 ppmw S and comprised of diverse sulfur compositions. In fixed bed continuous adsorption tests, 4 wt.%Ag/TiO$_x$–Al$_2$O$_3$ demonstrated saturation capacities of 10.11, 6.11, and 7.4 mg S/g adsorbent for JP5 (1172 ppmw S), JP8 (630 ppmw S), and ORD (452 ppmw S), respectively. In equilibrium saturation experiments, the adsorbent was able to desulfurize ULSD down to less than 75 ppbw S and this was achievable even when the initial concentration of non-sulfur aromatics was greater than 25,000 times higher. Dispersing TiO$_x$ onto high surface area alumina and silica substrates increased the sulfur adsorption capacities of both. This enhancement in adsorption capacity increased still further with silver addition. Higher Ag loading (up to ∼12 wt.%Ag) on TiO$_x$–Al$_2$O$_3$ proved beneficial to sulfur adsorption capacity when compared to TiO$_2$ (up to ∼4 wt.%Ag), indicating that the mixed oxide supports were able to host more active silver oxides. The adsorption selectivity toward different sulfur compounds present in the fuels varied during the fixed bed adsorption tests. The adsorbent had the greatest affinity for BT's and the least for TMBT's and DMDBT's (the selectivity order from the strongest to weakest adsorption was: BT > MBT > DMBT > DBT ≈ MDBT > TMBT ≈ DMDBT). Ag/TiO$_x$–Al$_2$O$_3$ was thermally regenerable in air for multiple cycles at temperatures ranging from 110 to 450 °C. The effects of titanium loading, silver loading, and titanium precursor on sulfur adsorption capacity are also presented.

© 2012 Elsevier Ltd. All rights reserved.

1. Introduction

Sulfur and its derivatives are major contaminants in hydrocarbon fuels. Desulfurization of fuels has gained importance due to environmental concerns, and many countries are enacting laws limiting maximum sulfur emissions. For example, the maximum sulfur concentration in highway diesel in the US has been limited to 15 ppmw since 2006, down from 500 ppmw [1–3]. Other transportation fuels are also being regulated to reduce sulfur content.

Desulfurization also has a significant impact on the successful application of fuel cell technologies. Transportation fuels such as gasoline, diesel, and jet fuel are ideal for on-board fuel cell systems because of their high energy density, availability, and operational safety factors. However, the development of fuel cell systems is restricted due to the demand of ultra low sulfur feeds in their reformation systems [4]. Sulfur poisons precious metal electrodes in fuel cells and reforming catalysts, therefore only fuels with less than 100 ppb sulfur content are allowable in fuel cell systems such as Proton Exchange Membrane (PEM) fuel cells [1,5]. High temperature Solid Oxide Fuel Cells (SOFCs) typically require less than 30 ppm S in the feed prior to reforming [6].

Most of the organosulfur compounds are generally removed from hydrocarbon fuels by conventional Hydrodesulfurization (HDS) process in refineries. It is a catalytic process requiring high temperature (300–400 °C) and pressure (3–6 MPa) in the presence of hydrogen [1]. In the recent years, refineries are facing higher amounts of sulfurous crude oil as feedstock due to the diminishing crude oil reserves and producing larger volume of products from high sulfur heavy oil fractions. This, along with the demand for ultra clean fuel, are increasing the desulfurization cost [7]. Especially for achieving the sulfur concentration tolerable to fuel cells, the HDS process has to increase its reactor volume and H_2 consumption [8,9]. HDS also has less satisfactory performance in removing Poly Aromatic Sulfur Heterocycles (PASHs) [10]. Hence, it is necessary to develop an alternative or supplementary process to HDS for deep desulfurizing fuel. Among several alternative processes reported earlier [1,8,11–17], desulfurization by direct adsorption of organosulfur species at ambient conditions has gained much attention [9,18–24]. Adsorptive desulfurization provides great applicability and has several advantages such as its selectivity toward PASH, scalability, and the ability to desulfurize hydrocarbon fuels to near zero sulfur content. It also does not require hydrogen or any other auxiliary units. Adsorptive desulfurization can supplement HDS process as a polishing step and offers an alternative solution to the high cost of producing ultra clean fuels.

The adsorption lab at the Auburn University Center for Microfibrous Materials Manufacturing (CM3) has developed a silver based adsorbent for the desulfurization of high sulfur refined fuels at room temperatures [25,26]. It is one of the few adsorbents reported in the literature that can reduce sulfur down to ppmw level in "oxidized" form without requiring any sulfidation or activation. After characterizing the adsorbent via X-ray Photoelectron Spectroscopy (XPS) and Electron Spin Resonance (ESR), silver (I) oxide was observed to be the active phase for sulfur adsorption [27]. Metal oxide supports, especially TiO_2, had significant contribution to the overall sulfur adsorption capacity in addition to the silver active sites [28]. The "active sites" on the supports were believed to be the surface acid sites that were generated during calcination in air at higher temperatures [29–31]. Titanium oxide has shown to be a better support for silver than other common metal oxide supports not only for the presence but also for the concentration of surface acid sites. The active sites on titania also causes better metal dispersion than other surfaces [26]. In spite of these features, TiO_2 is not available in high surface area as compared to most other commercial metal oxide supports for which the overall sulfur adsorption capacity is low. In addition, the silver loading on titania is confined to only 4 wt.% above which causes particle agglomeration and reduction in silver oxide fraction thereby lowering sulfur adsorption capacity [26]. Assessing these problems, we tried to increase active titanium oxide surface area.

One possible way of increasing titanium oxide surface area is to disperse it onto high surface area supports such as SiO_2, Al_2O_3, activated carbon, and zeolites. Mixed metal oxide supports containing titanium oxide have been widely reported in the literature [30–36]. Titanium oxide modified supports have higher concentration of coordinative unsaturated sites [35]. The addition of titanium oxide on alumina resulted in greater number and strength of surface acid sites [30,37]. Silver has been successfully applied on these mixed oxide supports for other applications such as dehydrogenation of methanol [38]. If high surface area supports are decorated with titanium oxide functional groups, it may increase the active area for sulfur adsorption. Increase in overall surface area may also facilitate in loading of higher amount of oxidized silver. All these changes may result in higher sulfur adsorption capacity.

The previous works conducted at CM3-adsorption lab were focused primarily on desulfurizing high sulfur jet fuels (JP5 and JP8). It is known that the sulfur compositions in hydrocarbon fuels vary widely with respect to their volatility cuts. The sulfur concentration and the type of sulfur compounds present would obviously affect the adsorbent capacity and selectivity. Therefore it is necessary to study the effect of various types of organosulfur compounds on sulfur adsorption.

The objective of this work was to study the performance of silver adsorbents supported on titanium oxide dispersed mixed oxides for desulfurizing challenge fuels comprised of various sulfur compounds. TiO_x–Al_2O_3 and TiO_x–SiO_2 mixed oxide supports were prepared and silver was supported on these materials. The adsorbents were tested in desulfurizing JP5, JP8, Off-Road Diesel (ORD) and Ultra Low Sulfur Diesel (ULSD). The effects of titanium and silver loading were also investigated by means of desulfurization experiments. The effect of titanium precursor was studied by testing TiO_x–Al_2O_3 supports prepared by three different titanium precursors. Nitrogen physisorption was carried out to measure the BET surface area and pore volume. Breakthrough characteristics of the adsorbent for JP5, JP8, ORD, and ULSD challenge fuels were examined to assess the selectivity of the adsorbent toward different sulfur compounds present in refined fuels. The reasons behind varying selectivity were also discussed. Multi-cycle capability of Ag/TiO_x–Al_2O_3 was tested by regenerating saturated adsorbent in air at elevated temperatures. The surface topography of the adsorbent after regeneration was studied using Scanning Electron Microscopy (SEM).

2. Experimental

2.1. Adsorbent preparation

Gamma-Al_2O_3, Anatase–TiO_2 (Grade ST61120) and SiO_2 (Grade 21) were purchased from Alfa Aesar, Saint Gobain Norpro, and Grace Davison, respectively. All the supports were crushed and sieved to 850–1400 μm size followed by drying in a convection oven at 110 °C for at least 6 h before use. The precursors for titanium and silver were purchased from Alfa Aesar and were used as received. Benzothiophene (98%+) and *n*-octane (97%+) were acquired from Alfa Aesar and Acros Organics, respectively, and were used for model fuel preparation.

The blank supports used in desulfurization and characterization experiments were calcined in flowing air at 450 °C for 2 h before use. For the preparation of titanium oxide dispersed mixed oxide supports, titanium precursors were dispersed onto dried (at 110 °C for 6 h) Al_2O_3 and SiO_2 supports by means of incipient wetness method (dry impregnation). The concentrations of the solutions were such that the titanium metal loading was 10 wt.% at the time of impregnation. In other words, the Ti:Al and Ti:Si weight ratios were 1:4.4 and 1:3.9, respectively (unless specified otherwise). Three types of titanium precursors were used; titanium (IV) chloride 99% min, titanium isopropoxide 97%+, and titanyl (IV) oxide sulfate sulfuric acid hydrate ($TiOSO_4$). For solution preparation, titanium isopropoxide was dissolved in iso-propanol; titanyl oxide sulfate in water; and titanium (IV) chloride was used without any solvent. The supports were then dried in the convection oven at 110 °C for 6 h followed by calcination in flowing air in a tube furnace at 550 °C for 2 h. Based on previous works, the calcination temperature was optimized in terms of achieving complete conversion to titanium oxide and minimizing rutile formation [35,39–42].

Aqueous $AgNO_3$ was used as the silver precursor and was dispersed onto the supports by incipient wetness method (dry impregnation). The impregnated volume of the precursor solution was 100% of the pore volumes of the individual and mixed oxide supports, and its concentration was adjusted according to the desired metal loading on the supports. The samples were then dried

in the convection oven at 110 °C for 6 h followed by calcination in flowing air in a tube furnace at 450 °C for 2 h. The desulfurization capacities of different batches of the same formulation were within the error range of 10%.

2.2. Challenge fuels

JP5 and JP8 jet fuels were collected from NAVSEA Philadelphia and TARDEK, respectively. ORD and ULSD were acquired from local sources near Auburn, Alabama, USA. The initial sulfur contents of JP5, JP8, ORD, and ULSD were 1172, 630, 452, and 7.5 ppmw, respectively. The model fuel used in the fixed bed continuous adsorption experiments (breakthrough experiments) was prepared by mixing 3500(±25) ppmw benzothiophene (BT) with *n*-octane. Model fuel was employed in the experiments to compare the adsorbents with different metal loadings. The major sulfur species in the fuels were identified using analytical standards collected from Chiron AS.

2.3. Desulfurization experiments

For the desulfurization experiments, both static saturation tests and dynamic breakthrough tests were carried out in order to assess the sulfur adsorption capacities of the adsorbents. In the saturation experiments, JP5 and ULSD were used as the primary fuels. In each test, the fuel was mixed with the adsorbent and the mixture was agitated mechanically for 48 h. The fuel to adsorbent ratio was 20 ml of fuel per gram of adsorbent for JP5 and 10 ml of fuel per g of adsorbent for ULSD. The equilibrated fuel was analyzed to measure the outlet total sulfur content, which was used to calculate equilibrium sulfur adsorption capacity. The breakthrough experiments were conducted using JP5, JP8, ORD, ULSD, and model fuel. In each experiment, the adsorbent was loaded onto a quartz adsorber in a vertical packed column configuration and was supported on both sides by quartz wool. The bed weight, diameter, and volume were 10 g, 1.6 cm, and 15–16 cm^3, respectively. The adsorbents were not activated prior to the experiment. Fuel flowed upward vertically with a flow rate of 0.5 ml/min and WHSV of 2.5 h^{-1} (LHSV ∼ 2 h^{-1}) using a peristaltic pump. Upward flow minimized bed channeling and ensured complete wetting of all adsorbent particles. Both saturation and breakthrough experiments were performed at room temperature and atmospheric pressure. Outlet fuel was sampled at regular intervals and analyzed. The outlet sulfur concentration (C) was normalized by inlet sulfur concentration (C$_o$) and the breakthrough curves were obtained by plotting C/C$_o$ against time (minutes). The breakthrough capacity was calculated at the 10 ppmw sulfur threshold limit. For calculating the capacity at saturation, linear integration method was applied. For regeneration, the saturated bed was heated in flowing air at 110 °C for 1 h, followed by 230 °C for 2 h, and finally 450 °C for 1 h. After regeneration, the rejuvenated adsorbent bed was cooled down to room temperature and used again for breakthrough experiments in desulfurizing JP5.

2.4. Analysis of fuel

The total sulfur content of the fuel was measured using an Antek 9000S Total Sulfur Analyzer (TSA). The lower detection limit of TSA was measured to be 200 ppbw. To determine the sulfur content as well as sulfur speciation, fuel samples were analyzed in a Varian CP3800 Gas Chromatograph (GC) equipped with a Pulsed Flame Photometric Detector (PFPD). The GC used a Restek XTI-5 crossboard column of 30 m length and 0.25 mm ID. The sample injection volume was 1 μL with split ratios between 0 and 100. For analysis, the column temperature was initially at 100 °C for 3 min and was then raised to 300 °C at 10 °C/min and was kept

there for 2 min. Both GC-PFPD and TSA were calibrated using standard samples prepared by successive dilution of JP5, ORD, and also using model fuels containing octane-sulfur mixtures with known sulfur concentrations. Successive dilution of ULSD was also carried out to prepare standard solutions. Several solutions were prepared with sulfur content ranging from 75 ppbw to 7.5 ppmw. The solutions were used to calibrate the GC-PFPD so that it can measure ultra low concentration of sulfur (e.g. 75 ppbw).

2.5. Characterization

Nitrogen physisorption was conducted to calculate the BET surface areas, pore volumes, and average pore sizes of the adsorbents in a Quantachrome Autosorb AS1 analyzer. The analysis was carried out at −196 °C. Prior to the analysis, all the samples were outgassed at 150 °C for 2 h for moisture removal. The surface topography of fresh and regenerated adsorbents was acquired using a JOEL 7000-F Scanning Electron Microscope (SEM). The voltage of the equipment was 40 kV during imaging.

3. Results and discussion

3.1. Adsorbent formulation

3.1.1. Support comparison and characterization

The equilibrium saturation capacities of the commercial and the mixed oxide supports were evaluated through saturation experiments at room temperature and atmospheric pressure. Fig. 1 and Table 1 illustrate the comparison between the capacities of the supports that indicate considerable increase in sulfur adsorption capacities in the case of mixed oxide supports. TiO$_x$–Al$_2$O$_3$ support had higher capacity than individual anatase–TiO$_2$ or γ-Al$_2$O$_3$ supports. For TiO$_x$–SiO$_2$ support, the contribution of titanium oxide on sulfur adsorption capacity was higher. Table 1 shows the saturation capacities of the supports per unit area basis. Among the individual supports materials, titania had the highest saturation capacity per m^2 surface area but had the lowest overall surface area. The TiO$_x$–Al$_2$O$_3$ support had moderate capacity per unit area, but the overall saturation capacity was higher. It is important to note that instead of Y-zeolites; silica and alumina supports were used to reduce diffusion limitations during operations at ambient conditions.

Nitrogen physisorption tests reveal that there were significant changes in BET surface areas of the mixed oxide supports (Table 1). TiO$_x$–Al$_2$O$_3$ and TiO$_x$–SiO$_2$ supports had 54% and 97%
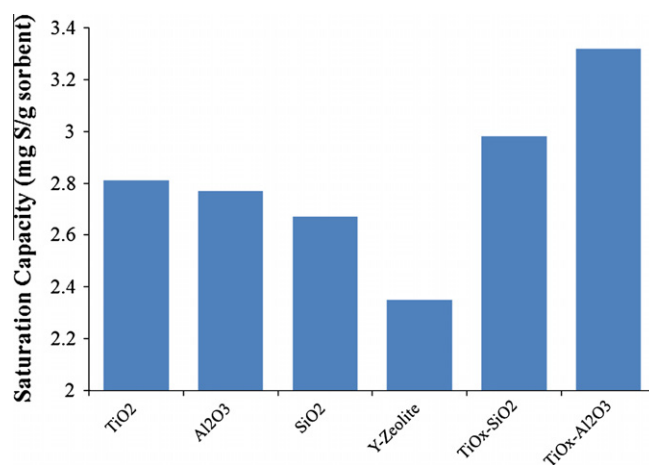

Fig. 1. Equilibrium saturation capacities of different metal oxide supports acquired from saturation experiments with JP5 (1172 ppmw S) for 48 h (fuel to adsorbent ratio: 20 ml/g).

Table 1
Surface properties and equilibrium saturation capacities (per unit area basis) of different metal oxide supports acquired from N_2 physisorption tests and 48 h saturation experiments with JP5 (1172 ppmw S).

Supports	BET surface area (m^2/g)	Pore volume (cc/g)	Capacity (mg S/g adsorbent)	Capacity (μg S/m^2 surface area)
TiO_2	154	0.41	2.81	18.25
Al_2O_3	267	1.12	2.77	10.37
SiO_2	319	1.06	2.67	8.37
Y-zeolite	660	0.83	2.35	3.56
TiO_x–Al_2O_3 (Ti:Al = 1:4.4)	237	0.75	3.32	14.01
TiO_x–SiO_2 (Ti:Si = 1:3.9)	304	0.80	2.98	9.80

Table 2
Surface properties and equilibrium saturation capacities of 4%Ag adsorbents supported on mixed oxide supports acquired from N_2 physisorption tests and 48 h saturation experiments with JP5 (1172 ppmw S).

Adsorbents	BET surface area (m^2/g)	Pore volume (ml/g)	Capacity (mg S/g adsorbent)	Capacity (μg S/m^2 surface area)
4%Ag/TiO_x–Al_2O_3 (Ti:Al = 1:4.4)	222	0.61	10.55	47.52
4%Ag/TiO_x–SiO_2 (Ti:Si = 1:3.9)	263	0.66	7.36	27.98
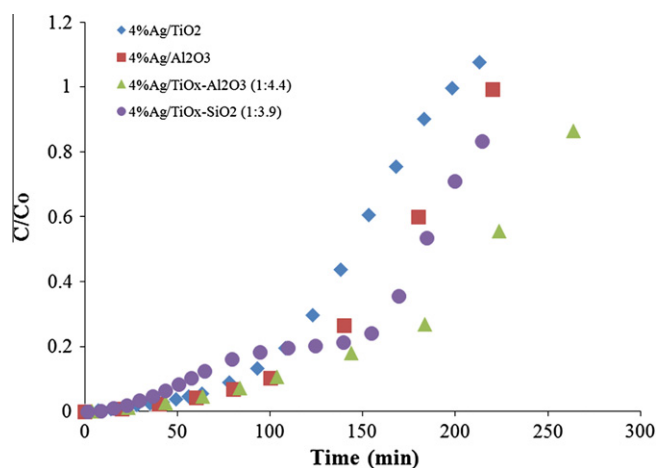
Fig. 2. Breakthrough performances of Ag loaded on titanium oxide dispersed supports and their comparisons with Ag loaded on individual supports (bed wt.: 10 g, WHSV: ~2.5 h^{-1}, fuel: JP5 – 1172 ppmw S).

more surface areas than TiO_2. The TiO_x–Al_2O_3 support had better desulfurization performance than TiO_x–SiO_2. Apparently there was better interaction between TiO_x and Al_2O_3 than that between TiO_x and SiO_2. Comparing the saturation capacities and BET surface areas of TiO_x–Al_2O_3 and Al_2O_3 supports, there was an increase of 3.64 μg S/m^2 surface area in sulfur adsorption capacity for TiO_x–Al_2O_3 support. To ascertain the extent of titanium oxide dispersion, the supports were examined via X-ray diffraction (XRD) where the graph of TiO_x–Al_2O_3 sample showed no titanium/anatase–TiO_2/rutile–TiO_2/brookite–TiO_2 peaks apart from the γ-alumina peaks (not shown here). This is common for mixed oxide supports, as observed by other researchers [30]. A similar scenario was also observed in the case of TiO_x–SiO_2 support. The probable explanations for this absence are either the titanium oxide particle size (anatase/rutile/brookite) is too small to be detected by XRD or titanium oxide is in some amorphous and disordered phase. Either way, it was evident that titanium phase was nanodispersed onto the supports. The measurement of titanium oxide active surface area in the mixed oxide supports and the study concerning interactions between titanium oxide and support materials are currently being pursued.

Mixed oxide supported silver adsorbents were tested in equilibrium saturation and breakthrough tests and were analyzed via N_2 physisorption. Silver loadings were 4% by weight for each sample.

The promotional effect of Ag addition was higher on mixed oxide supports than on individual supports. Table 2 shows the BET surface areas, pore volumes, and equilibrium saturation capacities of silver supported adsorbents from N_2 physisorption tests. The capacities were calculated from 48 h saturation experiments using a JP5 challenge (fuel to adsorbent ratio: 20 ml/g). The capacities of these two adsorbents were increased by 217% and 147%, respectively after Ag addition. Compared to the saturation capacity of 4%Ag/TiO_2, capacities of both the adsorbents were higher [26]. Fig. 2 exhibits the breakthrough performances of Ag/TiO_x–Al_2O_3 and Ag/TiO_x–SiO_2 and their comparison with Ag/TiO_2 and Ag/Al_2O_3 in fixed bed adsorption tests with JP5 as challenge fuels. The capacities at breakthrough (10 ppmw threshold limit) and at saturation of 4%Ag/TiO_x–Al_2O_3 were 0.90 and 10.11 mg S/g adsorbent, respectively. The capacities were higher when compared to 4%Ag/TiO_2 (0.79 and 5.65 mg S/g adsorbent). The 4%Ag/TiO_x–SiO_2 adsorbent had poor breakthrough capacity (0.67 mg S/g adsorbent), but had a decent saturation capacity (7.73 mg S/g adsorbent). So, Ag/TiO_x–Al_2O_3 and Ag/TiO_x–SiO_2 adsorbents had better desulfurization performances than Ag/TiO_2 and Ag/Al_2O_3 for JP5 challenge. The extent of silver (I) oxide present on these supports and the effect of surface acidity are currently under investigation.

3.1.2. Effect of support precursor

Precursors play a significant role in achieving desired phases of active centers for catalytic reactions and adsorption. Titanium oxide phases vary extensively for the types of precursor used and the preparation techniques. For sulfur adsorption from liquid fuels, the anatase form of titania appeared to perform better than rutile form. Hence, for preparation of titania dispersed supports, efforts were made to optimize the type of titanium precursors to achieve highest amount of anatase phase on the surface. For titanium, three types of precursors are commonly used: titanium isopropoxide, titanium (IV) chloride, and titanyl oxide sulfate [29,36,39,41,42]. There are also various methods of preparing mixed oxide supports, such as incipient wetness [35,43], sol–gel method [32,34], and atomic layer deposition [33,40]. However, in our case, incipient wetness method was purposefully employed because this method is simple and causes more presence of TiO_x on the support surface than the bulk phase [39]. Silver (4% by weight) impregnated on these supports were tested in breakthrough tests for desulfurizing JP5 (Fig. 3). Ag/TiO_x–Al_2O_3 adsorbent prepared by titanium isopropoxide had higher capacities at breakthrough (0.90 mg S/g adsorbent at 10 ppmw threshold limit) and at saturation (10.11 mg S/g adsorbent) than the other two (0, 5.89 mg S/g

adsorbent for titanyl oxide sulfate and 0.38, 7.92 mg S/g adsorbent for titanium chloride, respectively). This corresponds to the higher concentration of dispersed titanium oxide phase on the surface [30]. Besides precursor effect, the effect of impregnation sequence of Ag and Ti precursors was also tested, i.e. Ag was impregnated onto alumina support prior to Ti impregnation. The adsorbent had poor performance in sulfur adsorption.

3.1.3. Effect of titanium loading

The effect of titanium loading was also tested for sulfur adsorption. Fig. 4 illustrates the breakthrough characteristics of model fuel (3500 ppmw BT in *n*-octane) by adsorbent with different titanium loadings. The Ti:Al ratio by weight for the three samples during support preparation were 1:9.7, 1:4.4, and 1:2.6, that corresponds to 5%, 10%, and 15% Ti loading by weight on alumina support at the time of impregnation, respectively. The silver loading for these adsorbents was 12% by weight. The Ag/TiO$_x$–Al$_2$O$_3$ (Ti:Al = 1:4.4) adsorbent had the optimized loading of titanium oxide for sulfur adsorption, for which the capacities at breakthrough and at saturation were 10.67 and 12.23 mg S/g adsorbent, respectively. Higher Ti loading caused pore blockage and reduced surface area that offset the increase in titanium oxide concentration.
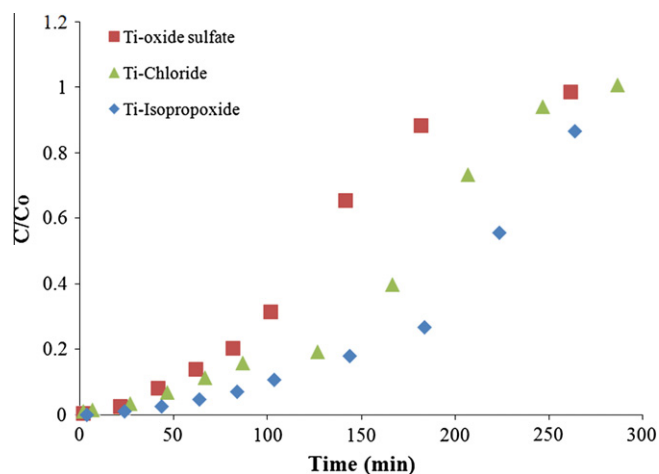
3.1.4. Effect of silver loading

One of the objectives of this work was to facilitate higher silver loading in active form by increasing titanium oxide surface area. The effect of silver loading was studied on TiO$_x$–Al$_2$O$_3$ support to test this. Fig. 5 illustrates the breakthrough of sulfur in JP5 (1172 ppmw sulfur) using TiO$_x$–Al$_2$O$_3$ (Ti:Al = 1:4.4 by weight) impregnated with 4%, 8%, 12%, and 16% silver by weight. Up to 12 wt.%Ag loading on TiO$_x$–Al$_2$O$_3$ was beneficial to sulfur adsorption, with breakthrough (at 10 ppmw threshold) and saturation capacities of 1.51 and 12.73 mg S/g adsorbent, respectively. This was up from 4 wt.% for Ag on TiO$_2$ support implying the effect of higher surface area.

Previous studies conducted at CM3 reported development of pore clogging with increased Ag loading (more than 4 wt.%Ag) on TiO$_2$ support [26]. In this work, similar phenomenon was observed where the atomic utilization of silver was lower at higher loadings. The obstruction of sulfur active sites by large Ag particles was extremely significant in 16%Ag loaded adsorbent to affect the sulfur adsorption capacity. In this case, agglomeration of Ag led to the formation of large particles and lower Ag dispersion. The large Ag particles blocked the pores, thereby decreasing sulfur adsorption capacity, similar to Ag/TiO$_2$ adsorbents [26]. From these observations, the optimized Ag loading on TiO$_x$–Al$_2$O$_3$ mixed oxide supports were estimated to be ca. 10% by weight.

Fig. 3. Breakthrough performance comparison of 4%Ag supported on TiO$_x$–Al$_2$O$_3$ prepared from different titanium precursors (bed wt.: 10 g, WHSV: ~2.5 h^{-1}, fuel: JP5 – 1172 ppmw S).

Fig. 5. Breakthrough performance comparison of TiO$_x$–Al$_2$O$_3$ adsorbents with 4, 8, 12, and 16 wt.%Ag loading (bed wt.: 10 g, WHSV: ~2.5 h^{-1}, fuel: JP5 – 1172 ppmw S).
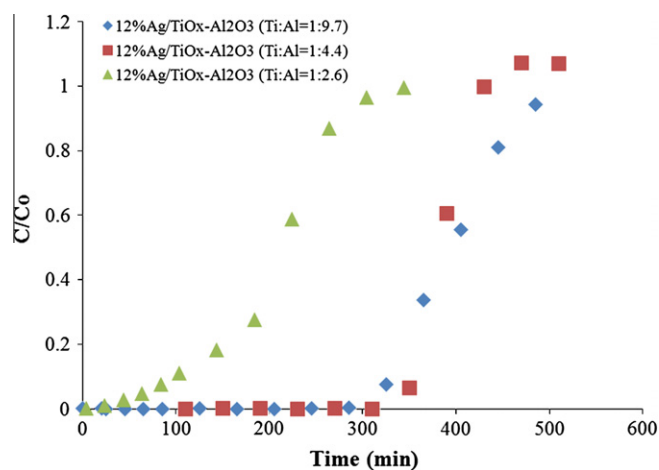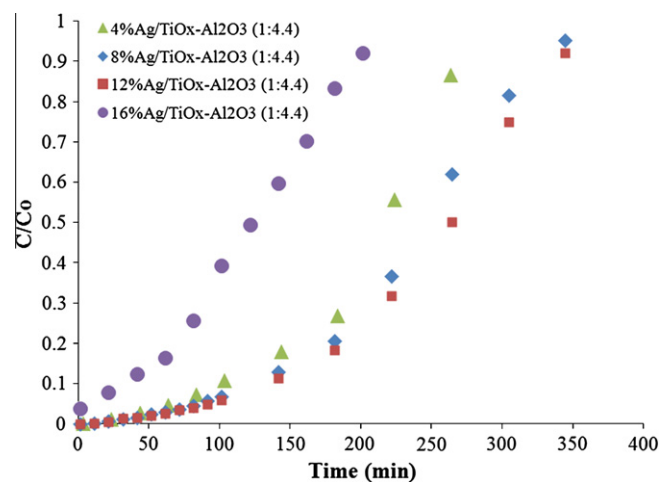

Fig. 4. Breakthrough performance comparison of 12%Ag supported on TiO$_x$–Al$_2$O$_3$ supports with varied titanium loadings (bed wt.: 10 g, WHSV: ~2.5 h^{-1}, fuel: model fuel – 3500 ppmw BT).
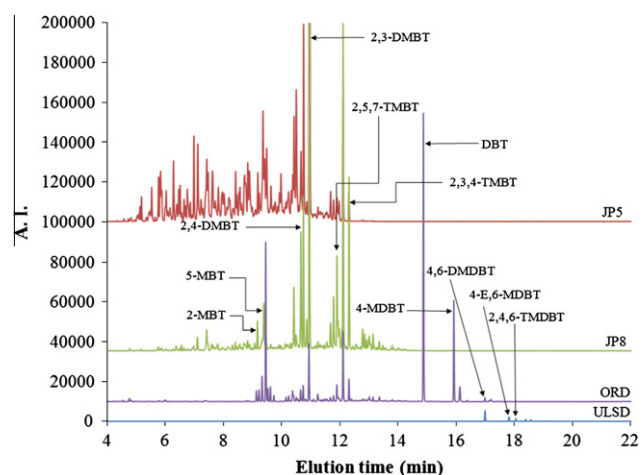

Fig. 6. GC-PFPD chromatograms of JP5 (1172 ppmw S), JP8 (630 ppmw S), ORD (452 ppmw S), and ULSD (7.5 ppmw S) exhibiting sulfur species present.
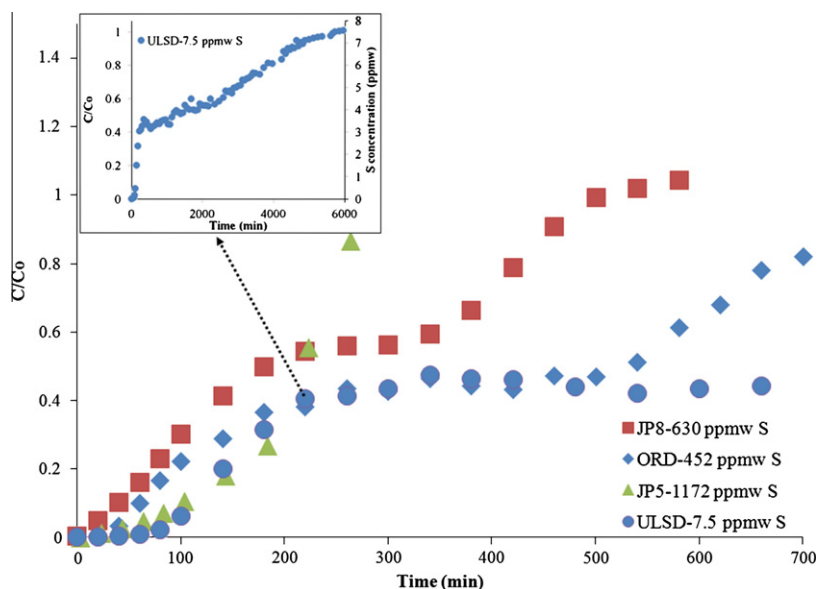
Fig. 7. Breakthrough performance comparison of 4%Ag/TiO$_x$–Al$_2$O$_3$ (Ti:Al = 1:4.4) for desulfurizing JP5, JP8, ORD, and ULSD (bed wt.: 10 g, WHSV: ~2.5 h^{-1}). Inset figure: extended breakthrough characteristics of ULSD challenge using 4%Ag/TiO$_x$–Al$_2$O$_3$ (Ti:Al = 1:4.4).

3.2. Effect of various sulfur compounds in commercial fuels

Commercial petroleum fuels have diverse mixtures of hydrocarbons considering their origin from different distillation fractions of crude oil in the refinery. Diversity in sulfur compounds is no exemption. The sulfur species can vary with respect to the number of aromatic rings and alkyl side chains attached to thiophene (T). These factors can affect the sulfur adsorption capacity. The PFPD chromatograms of Fig. 6 illustrate the sulfur peaks of JP5, JP8, ORD, and ULSD showing different sulfur species. As illustrated from the figure, JP5 and JP8 contain almost similar sulfur compound, although JP8 contains more trimethyl benzothiophenes (TMBT). JP5 and JP8 have approximately 9% and 29% of the total sulfur compounds as TMBT's, respectively. Generally diesel is generated from the heavier fractions of crude oil. As a result, it contains greater quantities of aromatic compounds and also heavier sulfur heterocycles. The chromatogram depicts that dibenzothiophene (DBT) derivatives constitute significant portion of the sulfur species in ORD, majority of which were DBT and 4-methyl dibenzothiophene (4-MDBT). Other than ORD, ULSD also contains substituted DBT as sulfur heterocycles, among which 4, 6-DMDBT is the major sulfur compound. The organosulfur compounds in ULSD are the most refractory sulfur species present in petroleum fuels. Silver based adsorbents have different capacities for these thiophenic compounds as observed earlier using model fuels [28]. In addition, there are high concentrations of aromatic hydrocarbons and additives in these refined fuels that also compete for the active sites on the acid adsorbents. In case of ULSD, the concentration of non-sulfur aromatics is >25,000 times higher than that of sulfur heterocycles. This overwhelming concentration of non-sulfur heterocycles may have a significant effect on sulfur adsorption. The effect can also be observed from the difference in breakthrough capacities of the adsorbent for model fuel and JP5 (10.67 and 1.51 mg S/g adsorbent). In this case, the structure of different organosulfur compounds and the presence of different non-sulfur heterocycles adversely affected the breakthrough capacity. It is therefore necessary to gauge the influence of these factors through performance comparison between different commercial and logistic fuels.

The fuels were used as challenges in breakthrough experiments using 4%Ag/TiO$_x$–Al$_2$O$_3$ (Ti:Al = 1:4.4) adsorbent. Their breakthrough characteristics and sulfur adsorption capacities are shown

Table 3
Sulfur adsorption capacities for 4%Ag/TiO$_x$–Al$_2$O$_3$ (Ti:Al = 1:4.4) adsorbent for JP5 (1172 ppmw S), JP8 (630 ppmw S), ORD (452 ppmw S), and ULSD (7.5 ppmw S).

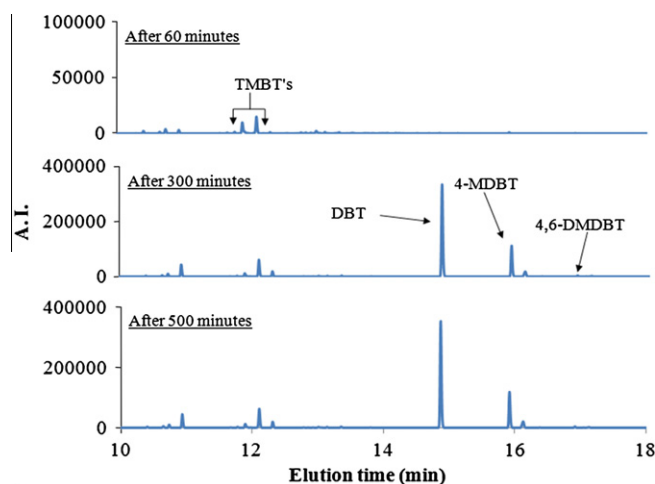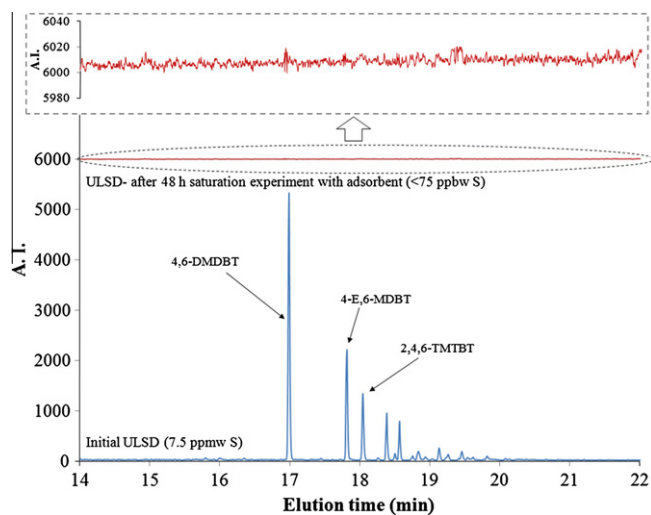| Fuel	Breakthrough capacity at 10 ppmw threshold limit (mg S/g adsorbent)	Capacity at saturation (mg S/g adsorbent)
JP5	0.9	10.11
JP8	0.12	6.11
ORD	0.64	7.40
ULSD	–[a]	0.59

[a] The initial sulfur content of ULSD was lower than 10 ppmw.

Fig. 8. GC-PFPD chromatograms of outlet ORD (452 ppmw S) sampled at 60, 300, and 500 min of breakthrough experiment with 4%Ag/TiO$_x$–Al$_2$O$_3$ (Ti:Al = 1:4.4) adsorbent; (bed wt.: 10 g, WHSV: ~2.5 h^{-1}).

in Fig. 7 and Table 3, respectively. The breakthrough capacity (calculated at 10 ppmw threshold limit) for JP5 (1172 ppmw sulfur) was the best among the fuels. However, JP5 was the quickest to saturate the adsorbent due to its higher initial sulfur content. For JP8, the curve broke initially but had a secondary breakthrough at around 350 min and $C/C_o \approx 0.55$ (outlet sulfur concentration ~ 350 ppmw S). Incoming methyl benzothiophene (MBT) was

Fig. 9. GC-PFPD chromatograms of ULSD before (below) and after (above) equilibrium saturation experiment using 4%Ag/TiO$_x$–Al$_2$O$_3$ (Ti:Al = 1:4.4) adsorbent (saturation time: 48 h, fuel to adsorbent ratio: 10 ml/g).

Fig. 10. Breakthrough performance comparison of fresh and regenerated 12%Ag/TiO$_x$–Al$_2$O$_3$ (Ti:Al = 1:4.4) adsorbents for five cycles (bed wt.: 10 g, WHSV: ~2.5 h^{-1}, fuel: JP5 – 1172 ppmw S).
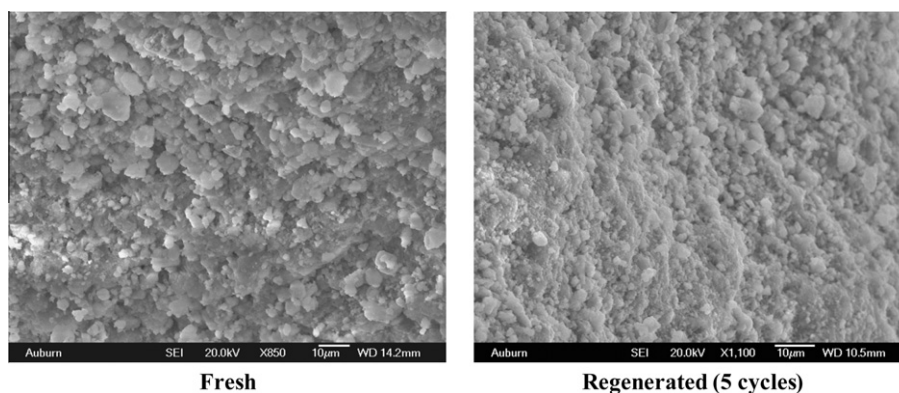
though in this case at around 500 min and $C/C_o \approx 0.45$ (outlet sulfur concentration $\sim$ 200 ppmw). Fig. 8 demonstrates the GC-PFPD chromatograms of outlet ORD samples at different times of breakthrough. Initially, sterically hindered TMBT's were the first group of sulfur species breaking through (at 60 min). DBT and 4-MDBT were the following ones as seen from the chromatogram at 300 min. However, the chromatogram of outlet ORD at 500 min (Fig. 8) shows that the adsorbent was slowly saturated with these compounds. The reason for this might be the replacement of the adsorbed aromatic compounds by DBT and its derivatives. The adsorbent continued to adsorb the entire inlet MBT's till saturation.

The sulfur adsorption capacity of 4%Ag/TiO$_x$–Al$_2$O$_3$ (Ti:Al = 1:4.4) for ULSD was significantly lower than those of the jet fuels and ORD. The possible reasons for this are the low initial sulfur concentration of ULSD and the effect of aromatic hydrocarbons and heteroatoms competing for the adsorption sites. The methyl groups in DBT derivatives e.g. 4, 6-DMDBT caused steric hindrances to adsorption on the metal cations. However, the surface acid sites (hydroxyl groups) were able to adsorb the sulfur compounds. The breakthrough curve leveled off at $C/C_o \approx 0.5$–0.6 and stayed in this range till 2000 min or 100 ml fuel/g adsorbent (shown in-set of Fig. 7). The adsorbent continued to adsorb till 6000 min or 300 ml fuel/g adsorbent. Plausible explanation for this might be the replacement of adsorbed aromatic hydrocarbons by incoming sulfur compounds. In the breakthrough tests, the adsorbent had the greatest affinity for BT's and the least for TMBT's and DMDBT's. The adsorbent selectivity order from the strongest to weakest adsorption was observed to be: BT > MBT > DMDBT > DBT $\approx$ MDBT > TMBT $\approx$ DMDBT. Identification of the sites active for sterically hindered sulfur species and the estimation of adsorption energies are currently being pursued.

Equilibrium saturation experiment using 4%Ag/TiO$_x$–Al$_2$O$_3$ (Ti:Al = 1:4.4) with a ULSD challenge was carried out where the fuel to adsorbent ratio was 10 ml/g. The GC-PFPD chromatograms in Fig. 9 show the sulfur species present in ULSD before and after saturation experiment. The sulfur species were undetectable in the fuel after saturation as shown from the chromatogram. The lower detection limit calibrated for the GC-PFPD method in split-less mode was 75 ppbw. So, the adsorbent was able to remove >99% of the sulfur species and desulfurize ULSD to almost zero sulfur content. This demonstrates the excellent selectivity of the adsorbent towards thiophenic sulfur compounds.

3.3. Regeneration

The regenerability of silver adsorbent supported on TiO$_x$–Al$_2$O$_3$ was tested by heating the saturated adsorbent bed in flowing air. The temperature was slowly ramped to ensure appropriate evacuation of hydrocarbons and PASH residues from the adsorbent bed.

preferentially adsorbed while more sterically hindered BT (e.g. TMBT's) remained in outlet fuel. Secondary breakthrough marks the saturation of adsorbent by MBT's. In the case of ORD, the curve broke early and had a secondary breakthrough similar to JP8;

Fresh

Regenerated (5 cycles)

Fig. 11. SEM images of fresh and regenerated (after five cycles) 12%Ag/TiO$_x$–Al$_2$O$_3$ (Ti:Al = 1:4.4) adsorbent.

After this, the bed was cooled down and tested again in breakthrough tests. The adsorbent was taken through five cycles of adsorption–regeneration using JP5. Fig. 10 illustrates the breakthrough curves for fresh and regenerated 12%Ag/TiO$_x$–Al$_2$O$_3$ (Ti:Al = 1:4.4) adsorbents. The breakthrough performance was consistent for multiple cycles. To check the surface topography of the adsorbent after regeneration, the samples were studies via SEM. Fig. 11 shows the SEM images of fresh and regenerated adsorbent after five cycles. No significant difference could be seen between the two samples, indicating stability in multi cycle heat treatment. Usually for supported metal catalysts, especially supported on γ-alumina, multiple heat treatment can cause metal sintering, thereby reducing activity. The phenomenon was not observed here, implying that titanium oxide stabilizes silver oxide phase interacting with alumina [44].

4. Conclusions

Silver on TiO$_x$–Al$_2$O$_3$ and TiO$_x$–SiO$_2$ mixed oxide supports were observed to be effective sulfur adsorbents for both high and low sulfur containing fuels. The adsorbents enhanced the sulfur adsorption capacity (mg S/g adsorbent) and lowered the exit sulfur threshold (ppmw S). In continuous breakthrough experiments, 4%Ag/TiO$_x$–Al$_2$O$_3$ (Ti:Al = 1:4.4) demonstrated saturation capacities of 10.11, 6.11, and 7.40 mg S/g adsorbent for JP5 (1172 ppmw S), JP8 (630 ppmw S), and ORD (452 ppmw S), respectively. The adsorbent was able to desulfurize ULSD (7.5 ppmw S) down to less than 75 ppbw S in the saturation experiments. Incorporation of TiO$_x$ onto high surface area Al$_2$O$_3$ and SiO$_2$ increased the number of sulfur adsorption sites. The mixed oxide supports were also able to host more silver oxides (up to ∼12 wt.%Ag) as demonstrated by the increase in capacity. The 12%Ag/TiO$_x$–Al$_2$O$_3$ (Ti:Al = 1:4.4) adsorbent had a saturation capacity of 12.73 mg S/g adsorbent for a JP5 challenge in breakthrough experiments. Differences in desulfurization performance were observed for different fuels and attributed to variations in organosulfur species. Methyl and ethyl groups attached to thiophenic derivatives created steric hindrances to adsorption on the silver cations. After examining the breakthrough performance of 4%Ag/TiO$_x$–Al$_2$O$_3$, the order of adsorption affinity toward the sulfur species (from the strongest to weakest adsorption) was observed to be: BT > MBT > DMDBT > DBT ≈ MDBT > TMBT ≈ DMDBT (based on their order of appearance at the bed outlet). The adsorbent maintained its capacity and stability after multiple cycles of adsorption-regeneration operations with JP5 challenge. Thus, silver on mixed oxide supports would provide better efficacy by enhancing the capacity and the extent of desulfurization while maintaining regenerability, scalability, and operability at ambient conditions. Future work will focus on the characterization of the adsorbents and on the mechanism for the adsorption of sulfur heterocycles at ambient conditions.

Acknowledgements

References

[1] Song CS. An overview of new approaches to deep desulfurization for ultra-clean gasoline, diesel fuel and jet fuel. Catal Today 2003;86:211–63.

[2] Pawelec B, Navarro RM, Campos-Martin JM, Fierro JLG. Towards near zero-sulfur liquid fuels: a perspective review. Catal Sci Technol 2011;1:23–42.

[3] Stanislaus A, Marafi A, Rana MS. Recent advances in the science and technology of ultra low sulfur diesel (ULSD) production. Catal. Today 2010;153:1–68.

[4] Shekhawat D, Spivey JJ, Berry DA. Fuel cells: technologies for fuel processing. Spain: Elsevier; 2011.

[5] Song CS. Fuel processing for low-temperature and high-temperature fuel cells - challenges, and opportunities for sustainable development in the 21st century. Catal Today 2002;77:17–49.

[6] Velu S, Ma XL, Song CS, Namazian M, Sethuraman S, Venkataraman G. Desulfurization of JP-8 jet fuel by selective adsorption over a Ni-based adsorbent for micro solid oxide fuel cells. Energy Fuels 2005;19:1116–25.

[7] Bej SK, Maity SK, Turaga UT. Search for an efficient 4,6-DMDBT hydrodesulfurization catalyst: a review of recent studies. Energy Fuels 2004;18:1227–37.

[8] Babich IV, Moulijn JA. Science and technology of novel processes for deep desulfurization of oil refinery streams: a review. Fuel 2003;82:607–31.

[9] Sentorun-Shalaby C, Saha SK, Ma XL, Song CS. Mesoporous-molecular-sieve-supported nickel sorbents for adsorptive desulfurization of commercial ultra-low-sulfur diesel fuel. Appl Catal B – Environ 2011;101:718–26.

[10] Gates BC, Topsoe H. Reactivities in deep catalytic hydrodesulfurization: Challenges, opportunities, and the importance of 4-methyldibenzothiophene and 4,6-dimethyldibenzothiophene. Polyhedron 1997;16:3213–7.

[11] Seredych M, Lison J, Jans U, Bandosz TJ. Textural and chemical factors affecting adsorption capacity of activated carbon in highly efficient desulfurization of diesel fuel. Carbon 2009;47:2491–500.

[12] Chica A, Strohmaier K, Iglesia E. Adsorption, desorption, and conversion of thiophene on H-ZSM5. Langmuir 2004;20:10982–91.

[13] Yang RT, Hernandez-Maldonado AJ, Yang FH. Desulfurization of transportation fuels with zeolites under ambient conditions. Science 2003;301:79–81.

[14] Deshpande A, Bassi A, Prakash A. Ultrasound-assisted, base-catalyzed oxidation of 4,6-dimethyldibenzothiophene in a biphasic diesel-acetonitrile system. Energy Fuels 2005;19:28–34.

[15] Murata S, Murata K, Kidena K, Nomura M. A novel oxidative desulfurization system for diesel fuels with molecular oxygen in the presence of cobalt catalysts and aldehydes. Energy Fuels 2004;18:116–21.

[16] Grossman MJ, Lee MK, Prince RC, Garrett KK, George GN, Pickering IJ. Microbial desulfurization of a crude oil middle-distillate fraction: analysis of the extent of sulfur removal and the effect of removal on remaining sulfur. Appl Environ Microbiol 1999;65:3264 (vol. 65, p. 181, 1999).

[17] Mei H, Mei BW, Yen TF. A new method for obtaining ultra-low sulfur diesel fuel via ultrasound assisted oxidative desulfurization. Fuel 2003;82:405–14.

[18] Wang YH, Yang FH, Yang RT, Heinzel JM, Nickens AD. Desulfurization of high-sulfur jet fuel by pi-complexation with copper and palladium halide sorbents. Ind Eng Chem Res 2006;45:7649–55.

[19] Hernandez-Maldonado AJ, Qi GS, Yang RT. Desulfurization of commercial fuels by pi-complexation: monolayer CuCl/gamma-Al2O3. Appl Catal B – Environ 2005;61:212–8.

[20] Kim JH, Ma XL, Zhou AN, Song CS. Ultra-deep desulfurization and denitrogenation of diesel fuel by selective adsorption over three different adsorbents: a study on adsorptive selectivity and mechanism. Catal Today 2006;111:74–83.

[21] McKinley SG, Angelici RJ. Deep desulfurization by selective adsorption of dibenzothiophenes on Ag+/SBA-15 and Ag+/SiO2. Chem Commun 2003:2620–1.

[22] Bhandari VM, Ko CH, Park JG, Han SS, Cho SH, Kim JN. Desulfurization of diesel using ion-exchanged zeolites. Chem Eng Sci 2006;61:2599–608.

[23] Weber G, Bellat JP, Benoit F, Paulin C, Limborg-Noetinger S, Thomas M. Adsorption equilibrium of light mercaptans on faujasites. Adsorpt–J Int Adsorpt Soc 2005;11:183–8.

[24] Tran DT, Dunbar ZW, Chu D. Regenerable sulfur adsorbent for liquid phase JP-8 fuel using gold/silica based materials. Int J Hydrogen Energy 2012;37:10430–4.

[25] Tatarchuk B, Yang H, Nair S. Silver-based sorbents. US Patent Application; 2008.

[26] Nair S, Tatarchuk BJ. Supported silver adsorbents for selective removal of sulfur species from hydrocarbon fuels. Fuel 2010;89:3218–25.

[27] Samokhvalov A, Nair S, Duin EC, Tatarchuk BJ. Surface characterization of Ag/Titania adsorbents. Appl Surf Sci 2010;256:3647–52.

[28] Nair S, Tatarchuk BJ. Characteristics of sulfur removal by silver-titania adsorbents at ambient conditions. Adsorpt–J Int Adsorpt Soc 2011;17:663–73.

[29] Ramirez J, Macias G, Cedeno L, Gutierrez-Alejandre A, Cuevas R, Castillo P. The role of titania in supported Mo, CoMo, NiMo, and NiW hydrodesulfurization catalysts: analysis of past and new evidences. Catal Today 2004;98:19–30.

[30] Walker GS, Williams E, Bhattacharya AK. Preparation and characterization of high surface area alumina-titania solid acids. J Mater Sci 1997;32:5583–92.

[31] Rana MS, Maity SK, Ancheyta J, Dhar GM, Rao T. TiO2–SiO2 supported hydrotreating catalysts: physico-chemical characterization and activities. Appl Catal A – Gen 2003;253:165–76.

[32] Kamaruddin S, Stephan D. The preparation of silica-titania core-shell particles and their impact as an alternative material to pure nano-titania photocatalysts. Catal Today 2011;161:53–8.

[33] Keranen J, Guimon C, Liskola E, Auroux A, Niinisto L. Atomic layer deposition and surface characterization of highly dispersed titania/silica-supported vanadia catalysts. Catal Today 2003;78:149–57.

[34] Grzechowiak JR, Wereszczako-Zielinska I, Mrozinska K. HDS and HDN activity of molybdenum and nickel-molybdenum catalysts supported on alumina–titania carriers. Catal Today 2007;119:23–30.

[35] Ramirez J, Rayo P, Gutierrez-Alejandre A, Ancheyta J, Rana MS. Analysis of the hydrotreatment of Maya heavy crude with NiMo catalysts supported on

TiO(2)-Al(2)O(3) binary oxides – effect of the incorporation method of Ti. Catal Today 2005;109:54–60.

[36] Chen LC, Tsai FR, Huang CM. Photocatalytic decolorization of methyl orange in aqueous medium of TiO_2 and Ag-TiO_2 immobilized on gamma-Al_2O_3. J Photochem Photobiol A – Chem 2005;170:7–14.

[37] Peri JB. Infrared study of adsorption of carbon dioxide, hydrogen chloride and other molecules on acid sites on dry silica–alumina and gamma–alumina. J Phys Chem 1966;70:3168–&.

[38] Liu Q, Cao Y, Dai WL, Deng JF. The oxidative dehydrogenation of methanol over a novel low-loading Ag/SiO_2–TiO_2 catalyst. Catal Lett 1998;55:87–91.

[39] Pophal C, Kameda F, Hoshino K, Yoshinaka S, Segawa K. Hydrodesulfurization of dibenzothiophene derivatives over TiO_2–Al_2O_3 supported sulfided molybdenum catalyst. Catal Today 1997;39:21–32.

[40] Yoshinaka S, Segawa K. Hydrodesulfurization of dibenzothiophenes over molybdenum catalyst supported on TiO_2–Al_2O_3. Catal Today 1998;45:293–8.

[41] Castillo R, Koch B, Ruiz P, Delmon B. Influence of preparation methods on the texture and structure of titania-supported on silica. J Mater Chem 1994;4:903–6.

[42] Hsu WP, Yu RC, Matijevic E. Paper whiteners.1. Titania coated silica. J Colloid Interface Sci 1993;156:56–65.

[43] Klimova T, Gutierrez O, Lizama L, Amezcua J. Advantages of ZrO(2)- and TiO(2)-SBA-15 mesostructured supports for hydrodesulfurization catalysts over pure TiO(2), ZrO(2) and SBA-15. Microporous Mesoporous Mater 2010;133:91–9.

[44] Lee MS, Lee GD, Hong SS. A synthesis of titanium dioxides prepared by reverse microemulsion method using nonionic surfactants with different hydrophilic group and their photocatalytic activity. J Ind Eng Chem 2003;9:412–8.